for fiber E. It is seen that for the SBS-suppression fiber, the Brillouin frequency shift changes greatly along the fiber—as much as 300 MHz within 30 km. By contrast, the changes in Brillouin frequency shifts for fibers A–D were not more than 6 MHz within 30 km. The Brillouin-frequency-shift change along the length in fibers A to D seems to be induced by residual strain during the fiber-drawing process.

The SBS threshold power P_{th} of the test fibers was measured at both 1.32 and 1.55 μm. The measured SBS threshold powers are listed in Table 1. SBS threshold power P_{th} is given[4] as approximately

$$P_{th} \cong 21 \frac{KA_{eff}}{gL_{eff}}, \quad (1)$$

where K is the polarization factor and g is the gain coefficient. L_{eff} represents the effective length, defined as $L_{eff} = 1 - \exp(-\alpha L)/\alpha$, where α is the fiber loss and L is the fiber length. A_{eff} is the effective core area, which is defined as πW^2, where W is the mode-field radius when the field distribution is expressed as Gaussian.

Figure 2 shows the relationship between P_{th} and A_{eff}/L_{eff} for the test fibers. It is found that P_{th} is proportional to A_{eff}/L_{eff} independent of wavelength, except for fiber E. The relationship between P_{th} and A_{eff}/L_{eff} was obtained from Fig. 2 as the following equation:

$$P_{th} = 1.08 \times 10^{-17} \left(\frac{A_{eff}}{L_{eff}}\right) W. \quad (2)$$

This result suggests that for fibers with uniform Brillouin frequency shift, P_{th} can be estimated from the fiber loss, fiber length, and mode field radius and that gain coefficient is almost independent of the wavelength. However, as seen from Fig. 2, the experimental P_{th} of fiber D is a little different from the estimated value. It was concluded from Fig. 1(a) that the SBS threshold power is affected by the nonuniformity of the Brillouin frequency shift along the fiber. This effect was clearly observed for the SBS-suppression fiber, as shown in Fig. 1(b), whose P_{th} is approximately three times as large as the value estimated by Eq. (2).

In conclusion, a simple equation for estimating the SBS threshold power was obtained for fibers with uniform Brillouin frequency shift by using two parameters, A_{eff} and L_{eff}, without regard to the wavelength. It has also been clarified experimentally that the nonuniformity of Brillouin frequency shift along the fiber has a great effect on the SBS threshold power.

1. M. Tateda, M. Ohashi, and K. Shiraki, in *Conference on Optical Fiber Communication/International Conference or Integrated Optics and Optical Fiber Communication*, 1993 Technical Digest Series, Vol. 4 (Optical Society of America, Washington, D.C., 1993), paper ThJ4.
2. A. Wada, T. Nozawa, D. Tanaka, T. Sakai, and R. Yamauchi, in *Proc. European Conference on Optical Communication*, 1991, paper M.B1.
3. T. Horiguchi and M. Tateda, J. Lightwave Technol. **LT-7**, 1170 (1989).
4. D. Cotter, Opt. Commun. **4**, 10 (1983).

WF3 9911 1:30 pm

Generation of synchronous ultrahigh-repetition-rate bright/dark pulse trains by using nonlinear beat-signal conversion techniques

A. B. Grudinin, D. J. Richardson, R. P. Chamberlin, L. Dong, D. N. Payne, *Optoelectronics Research Centre, Southampton University, Southampton, U.K.*

The generation and propagation of bright and dark soliton pulses is of great scientific interest with relevance to many futuristic telecommunication and optical-processing applications. Bright solitons have been the subject of intense experimental investigation; however, the experimental study of dark-pulse behavior has been limited. This situation is in no small

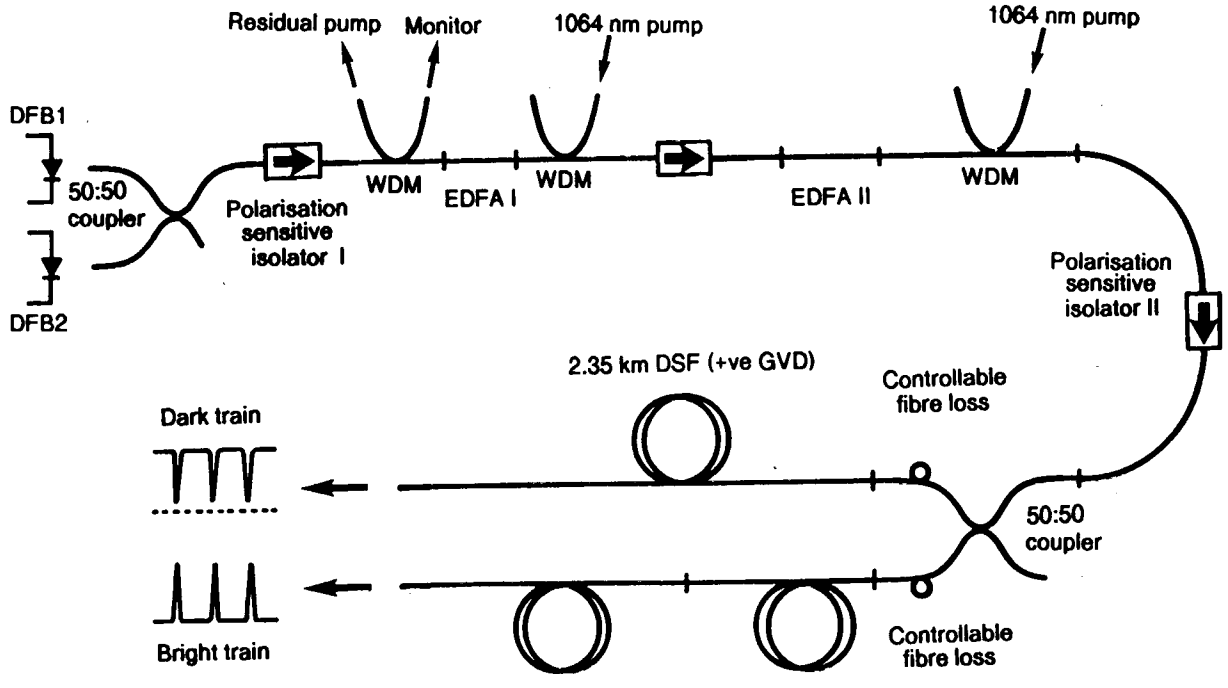

WF3 **Fig. 1.** Experimental configuration.

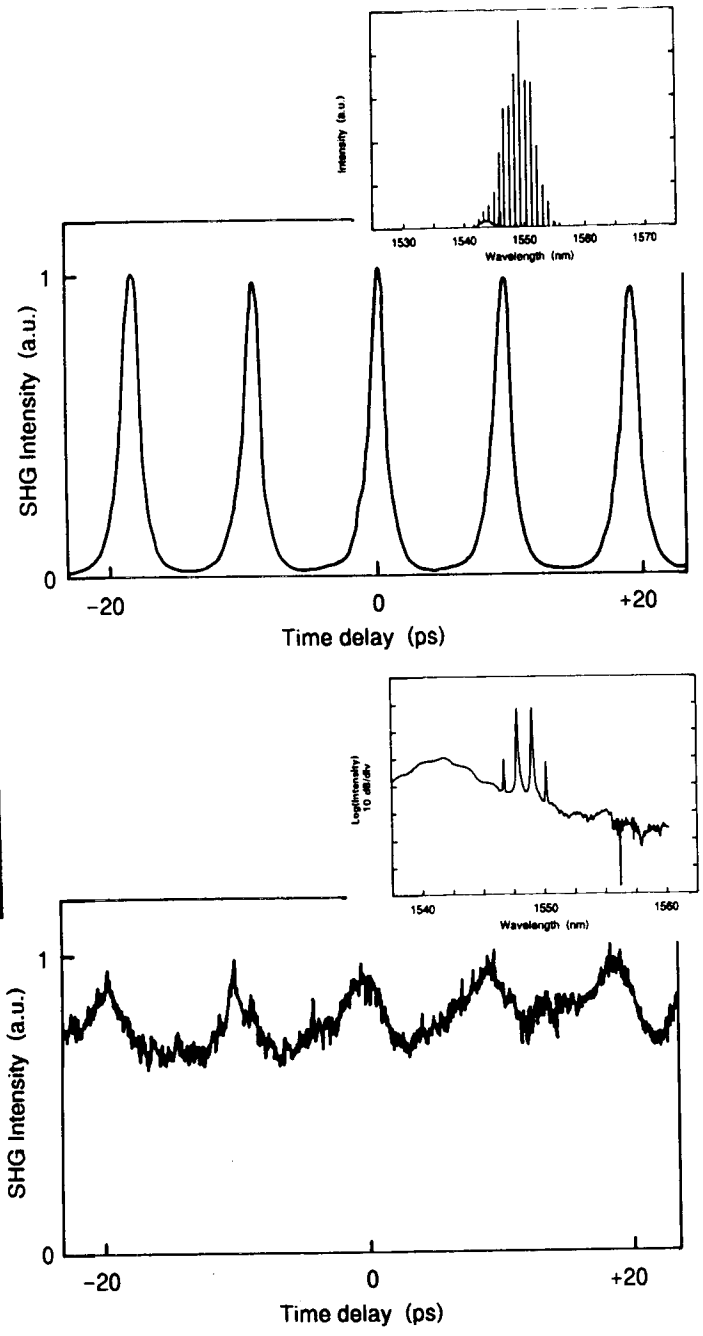

WF3 Fig. 2. Autocorrelation trace and optical spectrum of (a)110-GHz 800-fs bright soliton train and (b) 110-GHz dark pulse train.

part due to the difficulty of generating and measuring such pulse forms (see, e.g., Ref. 1 and the references therein).

In this work we describe a simple all-fiber synchronous source of both bright and dark pulses at 110 GHz based on nonlinear beat-signal transformation techniques. The bright and dark trains are formed by simultaneous parallel nonlinear propagation of a high-intensity beat signal in separate sections of dispersion-decreasing fiber[1] (DDF) and low-positive-GVD dispersion-shifted fiber[2] (DSF), respectively. The principle motivation behind developing such synchronous sources is that cross-correlation measurements between the dark and bright trains can easily be made, permitting detailed studies of high-frequency dark-pulse behavior.

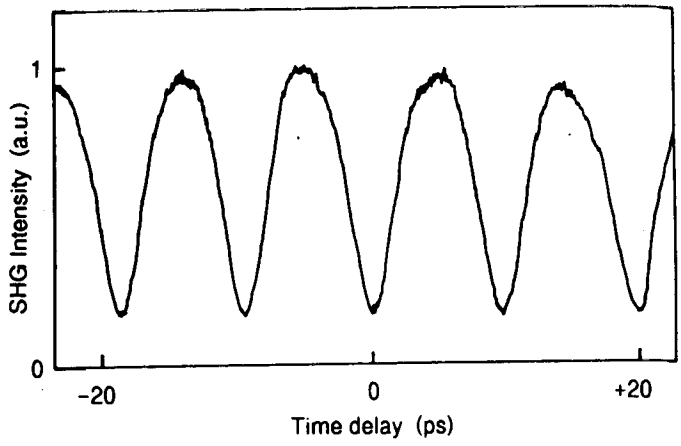

WF3 Fig. 3. Cross correlation of dark and bright pulse trains of Fig. 2.

The experimental configuration is illustrated in Fig. 1. Two single-frequency distributed-feedback (DFB) lasers operating around 1551 nm were combined by using a 50:50 coupler. The resulting beat signal (tuned to 110 GHz) was then passed through a two-stage 1064-nm-pumped Er^{3+}/Yb^{3+}-doped fiber amplifier. As much as 350 mW of average signal power was available at the amplifier output. The signal was then split by a coupler, 50% into the DDF (channel 1) for bright-soliton generation and 50% into the +GVD fiber (channel 2) for dark-pulse formation. Independent variation of the intensity in each channel could be effected by controlled bending of the fiber at the separate channel inputs.

Channel 1 consisted of 1100 m of low-GVD DSF (D = 0.5 ps nm^{-1} km^{-1}) followed by 1250 m of DDF with dispersion varying between 7 ps nm^{-1} km^{-1} at the fiber input and ≈0.5 ps nm^{-1} km^{-1} at the output. A typical autocorrelation trace and optical spectrum for the 110-GHz train of 800-fs pulses is shown in Fig. 2(a). The time–bandwidth product of the pulses was estimated to lie between 0.34 and 0.4, depending on the pump power, and was thus close to that expected for transform-limited $sech^2$ pulses.

Channel 2 consisted of 2350 m of −0.5-ps nm^{-1} km^{-1} (positively dispersive) DSF. The autocorrelation trace and spectrum of a dark pulse train are shown in Fig. 2(b) and clearly demonstrate the periodicity of the pulses (110 GHz). It is impossible, however, to make any further comments as to the temporal pulse quality from the autocorrelation alone because of the large background level between dark pulses.

The synchronous generation of both bright and dark pulses, however, permits cross-correlation measurements. The well-defined ultrashort bright solitons [Fig. 2(a)] can thus be used to probe the dark train [Fig. 2(b)]. The results are shown in Fig. 3, where a cross-correlation modulation depth of >80% is observed. The dark pulses are seen to have a width of approximately 2.4 ps (assuming a $sech^2$ form). At higher pump powers more complex pulse evolution was observed. Note that this particular dark pulse train is unstable and would decay on further propagation, as observed in Ref. 3. The use of alternative nonlinear beat-signal conversion techniques, such as propagation in +GVD DDF, should result in the generation of stable dark soliton pulses.

The measurements presented illustrate the great potential of this simple synchronous dual-output source for the generation and study of high-frequency dark-pulse propagation and interaction.

1. Y. S. Kishvar, IEEE J. Quantum Electron. **QE-29,** 250 (1993).
2. S. V. Chernikov, D. J. Richardson, R. I. Laming, D. N. Payne, and E. Dianov, Electron. Lett. **28,** 1210 (1992).
3. P. V. Mamyshev, P. G. Wigley, I. Wilson, and G. Stegeman, in *Conference on Quantum Electronics and Laser Science*, 1993 Technical Digest Series, Vol. 12 (Optical Society of America, Washington, D.C., 1993), paper QFH2.

WF4 1:45 pm

FDM three-channel fiber-optic low-frequency voltage sensor

L. Fabiny, S. T. Vohra, F. Bucholtz, A. Dandridge, *Optical Science Division, Code 5670, U.S. Naval Research Laboratory, Washington, D.C. 20375*

We report a frequency-division-multiplexed (FDM) three-channel fiber-optic low-frequency voltage sensor based on the electrostrictive effect. The high-resolution device is the first, to our knowledge, to demonstrate the measurement of three low-frequency voltage signals with a single fiber-optic interferometer and a single unmodulated laser. Measured cross talk between channels is less than −75 dB and is demonstrated to be a consequence of the nonlinear output of the interferometer for large optical phase shifts.

Electrostrictive materials are characterized by a quadratic relationship between the applied electric field E and the induced strain e, $e = ME^2$, where M is the electrostrictive coefficient. Fiber-optic (FO) interferometric dc and low-frequency voltage sensors exploit the nonlinear transducing properties of electrostrictive materials by mixing the voltage signal at frequency Ω with a carrier or dither at a much higher frequency ω ($\omega >> \Omega$), thereby upconverting the information of interest to a frequency region ($\omega \pm \Omega$) in which $1/f$ noise is not significant.[1] The nonlinear transduction mechanism is further exploited to demonstrate an FDM three-channel FO voltage sensor. Extension to multichannel operation ($N > 3$) is straightforward.

The three-channel FO Mach–Zehnder-interferometric low-frequency voltage sensor is shown in Fig. 1. The three electrostrictive transducers were of different mechanical characteristics, thereby allowing each to be driven at a carrier frequency near its mechanical resonance without interfering with the other transducers. As a test of the cross talk between sensors, each transducer also had a distinct low-frequency voltage

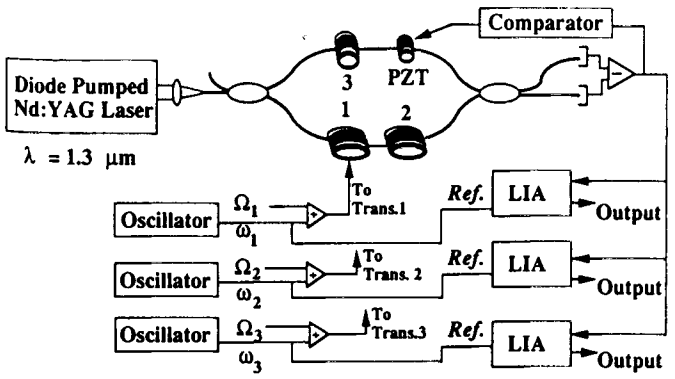

WF4 Fig. 1. Schematic diagram of the FDM three-channel fiber-optic voltage sensor.

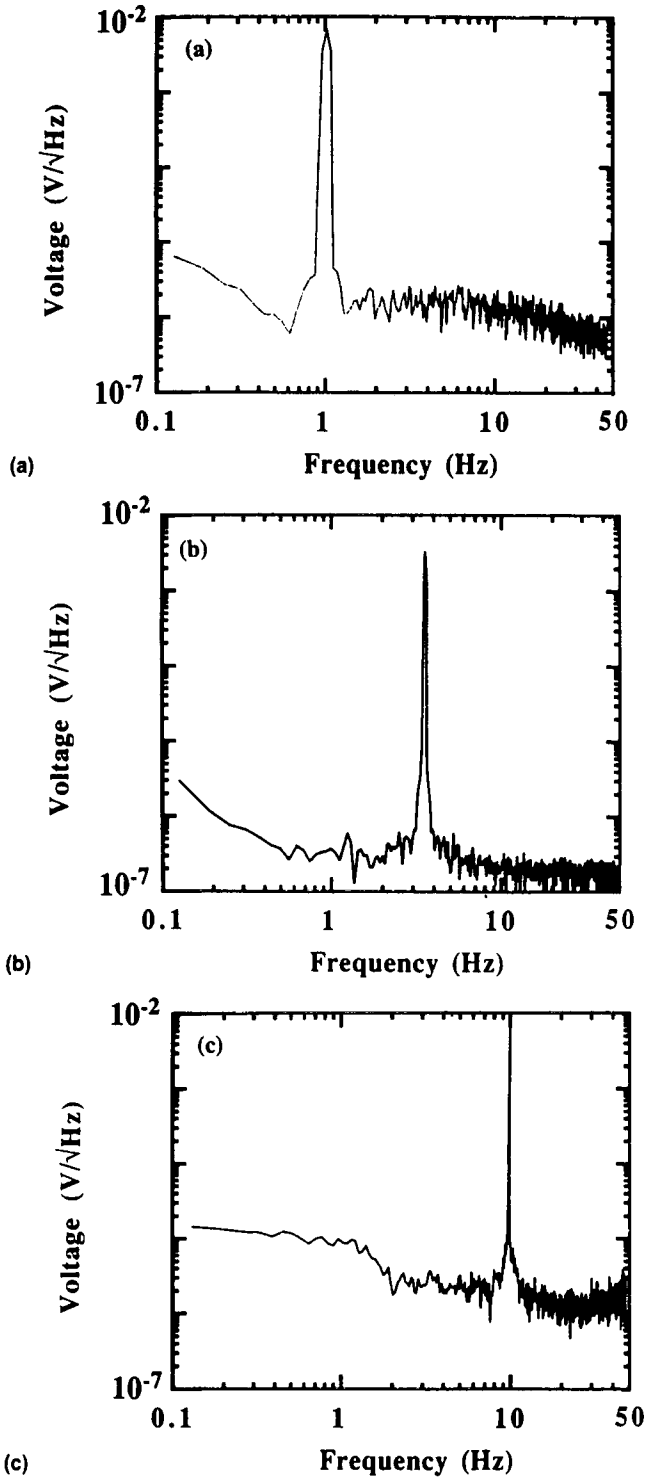

WF4 Fig. 2. Simultaneous output power spectra from the three lock-in amplifiers when low-frequency test signals are present: (a) channel 1, $\Omega_1/2\pi$ = 1.0 Hz, V_{Ω_1} = 3.2 mV; (b) channel 2, $\Omega_2/2\pi$ = 3.5 Hz, V_{Ω_2} = 1.3 mV; (c) channel 3, $\Omega_3/2\pi$ = 9.8 Hz, V_{Ω_3} = 4.7 mV.

signal applied, with $\Omega_1/2\pi$ = 1.0 Hz, $\Omega_2/2\pi$ = 3.5 Hz, and $\Omega_3/2\pi$ = 10 Hz. Three parallel phase-sensitive detectors were used to demodulate the output (Fig. 1), and an active homodyne technique was used to hold the interferometer at quadrature.

Power spectra from the outputs of the three lock-in amplifiers are shown in Figs. 2(a), 2(b), and (2c). We clearly ob-